



Mol Imaging Biol (2013) 15:585–595  
DOI: 10.1007/s11307-013-0634-y  
© World Molecular Imaging Society, 2013  
Published Online: 27 April 2013



## RESEARCH ARTICLE

# Development and Screening of Contrast Agents for *In Vivo* Imaging of Parkinson's Disease

Krista L. Neal,<sup>1</sup> Naomi B. Shakerdge,<sup>1</sup> Steven S. Hou,<sup>1</sup> William E. Klunk,<sup>2</sup>  
Chester A. Mathis,<sup>2</sup> Evgueni E. Nesterov,<sup>3,5</sup> Timothy M. Swager,<sup>3</sup> Pamela J. McLean,<sup>4</sup>  
Brian J. Bacskai<sup>1</sup>

<sup>1</sup>MassGeneral Institute of Neurodegenerative Disease, Massachusetts General Hospital, 114 16th Street, Charlestown, MA, 02129, USA

<sup>2</sup>Department of Psychiatry, University of Pittsburgh School of Medicine, Pittsburgh, PA, 15260, USA

<sup>3</sup>Department of Chemistry, Massachusetts Institute of Technology, Cambridge, MA, 02139, USA

<sup>4</sup>Department of Neuroscience, Mayo Clinic Florida, Jacksonville, FL, 32224, USA

<sup>5</sup>Department of Chemistry, Louisiana State University, Baton Rouge, LA, 70803, USA

### Abstract

**Purpose:** The goal was to identify molecular imaging probes that would enter the brain, selectively bind to Parkinson's disease (PD) pathology, and be detectable with one or more imaging modalities.

**Procedure:** A library of organic compounds was screened for the ability to bind hallmark pathology in human Parkinson's and Alzheimer's disease tissue, alpha-synuclein oligomers and inclusions in two cell culture models, and alpha-synuclein aggregates in cortical neurons of a transgenic mouse model. Finally, compounds were tested for blood–brain barrier permeability using intravital microscopy.

**Results:** Several lead compounds were identified that bound the human PD pathology, and some showed selectivity over Alzheimer's pathology. The cell culture models and transgenic mouse models that exhibit alpha-synuclein aggregation did not prove predictive for ligand binding. The compounds had favorable physicochemical properties, and several were brain permeable.

**Conclusions:** Future experiments will focus on more extensive evaluation of the lead compounds as PET ligands for clinical imaging of PD pathology.

**Key words:** Parkinson's disease, Dementia with Lewy bodies, Lewy bodies, Lewy Neurites, Alpha-Synuclein, Blood–brain barrier, *In vivo* imaging, Molecular imaging, PET

## Introduction

Parkinson's disease (PD) is the second most common neurodegenerative disorder. The prevalence of PD is

estimated at 1 % of people over 60 years of age and 0.3 % of the entire population. Despite the discovery of PD nearly 200 years ago, a clinical diagnosis is still the prevailing method to assess the disease [1]. PD is pathologically characterized by abnormal deposition of alpha-synuclein in multiple brain regions, specifically in the substantia nigra pars compacta in Lewy bodies (LB) and Lewy neurites (LN). These pathological features are thought to be upstream of several debilitating clinical symptoms, such as progressive bradykinesia, rigidity, and often a rest tremor [2].

Traditional CT and MRI imaging cannot detect PD pathology in the brain [2]. To date, there is no intrinsic

Electronic supplementary material The online version of this article (doi:10.1007/s11307-013-0634-y) contains supplementary material, which is available to authorized users.

Krista L. Neal and Naomi B. Shakerdge contributed equally to this work.

Correspondence to: Brian J. Bacskai; e-mail: [bbacskai@partners.org](mailto:bbacskai@partners.org)

contrast of alpha-synuclein or Lewy pathology that can be exploited for noninvasive imaging. Currently, radioligands are being used clinically to monitor the activity of the dopamine transporter (DaTSCAN) [3–5]. In PD, levels of dopamine in certain regions have been shown to be significantly reduced [6]. While these imaging agents may be of some benefit in monitoring or diagnosing PD, they are an indirect measure of the disease. A single-photon-emission PET imaging probe would be particularly useful for population-based epidemiological research, permitting early detection and therapeutic monitoring. Despite the development of exogenous biomarkers for other neurodegenerative diseases, there are no probes for the pathology of PD. An imaging biomarker of alpha-synuclein or Lewy pathology for PD would aid in allowing physicians to distinguish PD from other neurodegenerative diseases.

In the past decade, significant progress has been made in developing imaging biomarkers using positron emission tomography (PET) radiotracers for intracranial pathology. Pittsburgh Compound B (PiB) has been developed and evaluated for use in Alzheimer's disease (AD). The radiotracer labels amyloid pathology in animal models [7, 8] and in humans [9]. Recently, florbetapir has been approved for clinical amyloid imaging and shares physicochemical properties with PiB. Both reagents bind specifically to fibrillar beta-amyloid found in compact and cored plaques, a pathology that is present in several neurodegenerative diseases and the hallmark of AD [10].

The identification of an imaging agent specific to Lewy pathology, would greatly advance research for PD. The goal of this study was to identify an imaging probe for PD, analogous to PiB for AD. The main criteria for a successful imaging biomarker include: high affinity binding to Lewy body and Lewy neurite pathology; specificity to alpha-synuclein pathology over amyloid pathology, ability to traverse the blood–brain barrier (BBB) to access neuronal tissue, quick clearance of the compound not bound to Lewy pathology and the absence of radiolabeled metabolites in the brain [11]. Based on previous work screening AD-related imaging probes, a library of compounds was compiled that was selected based on good physicochemical properties for brain entry. The probes in this library, either novel or commercially available, are low molecular weight, uncharged, fluorescent, and rational candidates for BBB penetration and noninvasive imaging. These small molecule compounds were untested in their ability to bind PD pathology.

Several screening methods were used, both *in vitro* and *in vivo*, to characterize the compounds in our library with the goal of identifying suitable candidates for imaging ligands. The first screening method evaluated the ability to bind Lewy pathology in fixed human midbrain tissue from neuropathologically diagnosed DLB cases. This was considered the gold standard. In addition, two cell culture models were utilized, which overexpress alpha-synuclein and develop soluble oligomers or insoluble aggregates, with the

intention of developing a high-throughput screen to identify compounds that bind to the aggregated alpha-synuclein protein. Additionally, the ability of the compounds to label alpha-synuclein in the brain tissue of a transgenic mouse model, which overexpresses human alpha-synuclein in a subset of neurons, was evaluated. Finally, intravital microscopy tools were used to characterize the BBB penetration of the leading compounds in the intact mouse. Several lead compounds were identified which showed specificity for Lewy pathology, were able to cross the BBB, and will be evaluated further as suitable candidate PET ligands for clinical imaging in PD.

---

## Materials and Methods

### Materials

A library of over 100 fluorescent compounds that were either novel compounds or obtained from commercial sources was screened. LDS-722, LDS-759, LDS-798, LDS-730, Nile Blue 690 Cl04, H1TC Cl04, and Stilbene 420 were purchased from Exciton (Dayton, OH). THK-265 was obtained from Organica (Wolfen, Germany). 3-3'-Diethylthiadicarbocyanine iodide (33' DTDCI) was purchased from Sigma (St. Louis, MO). Nile red was purchased from Life Technologies (Invitrogen, Grand Island, NY). Novel imaging probes, RD-1 and NIAD-1, were synthesized by Dr. William Klunk at the University of Pittsburgh School of Medicine and Dr. Timothy Swager at Massachusetts Institute of Technology, respectively. Compounds were solubilized and stored as stock solutions in 100 % DMSO. Working solutions of each compound were diluted from stock with phosphate-buffered saline (PBS) to 500 nM, 2  $\mu$ M, and 5  $\mu$ M. General lab chemicals and cell culture supplies were purchased from Life Technologies (Invitrogen, Grand Island, NY). Synuclein monoclonal antibody H3C was a gift from Julia George (University of Illinois) and monoclonal anti-synuclein antibody was obtained from BD Biosciences (San Jose, CA). Alexa Fluor 488 secondary antibody was obtained from Jackson ImmunoResearch (West Grove, PA), and Cy5 fluorescent-conjugated secondary antibody from Invitrogen (Grand Island, NY).

### Animal Models

C57Bl/6J wildtype mice were obtained from Jackson Laboratory (Bar Harbor, ME, USA). Human recombinant synuclein-eGFP transgenic mice (Synuclein-GFP) were a gift from Eliezer Masliah (University of California San Diego). All experiments were conducted with approval of the Massachusetts General Hospital Animal Care and Use Committee and in compliance with NIH guidelines for the use of experimental animals.

### Human Tissue Collection

Postmortem midbrain tissue from DLB (Dementia with Lewy Bodies) and PD patients was obtained from the Harvard Brain Tissue Resource Center at McLean Hospital. Paraffin-embedded formalin-fixed tissue from the temporal lobe of AD patients was obtained through the Massachusetts Alzheimer's Disease Research

Center Brain Bank. The human brain tissue provided was neuropathologically defined as DLB tissue using standard criteria [12, 13].

### *LogP Estimates for Imaging Agents*

LogP was measured for the lead compounds using reverse phase C18 high-performance liquid chromatography (HPLC) as previously described [14]. Briefly, the retention time on an HPLC system (Phenomenex Prodigy ODS-3) with UV detection at 365 nm was measured using a fluorescence detector and the specific excitation and emissions peaks for each compound.

### *Labeling of Synuclein Pathology in Human DLB and PD Cases*

Blocks of midbrain tissue from human PD/DLB cases were fixed with 4 % paraformaldehyde and stored at  $-80^{\circ}\text{C}$ . In preparation for immunohistochemistry, the tissue block was deparaffinized with xylene and rehydrated. Midbrain tissue was sliced into 40- $\mu\text{m}$  thick sections with a freezing sledge Leica SM 2000R microtome. Free-floating tissue was permeabilized with 0.5 % Triton-X 100, then incubated with normal goat serum (NGS) at room temperature for 1 h with shaking. Primary H3C antibody (1:5,000 in 1.5 % NGS) to alpha-synuclein [15] was incubated overnight at  $4^{\circ}\text{C}$  with shaking, and then washed with 1X PBS three times. The tissue was then incubated for 2 h at room temperature with a fluorescent secondary antibody labeled with Alexa Fluor 488 or Cy5 (1:200 in PBS). Tissue was then treated with the compound to be tested. Each slice was incubated at room temperature for 30 min with either 500 nM, 2  $\mu\text{M}$ , or 5  $\mu\text{M}$  of compound dissolved in PBS. The tissue was rinsed with three washes of PBS, and then mounted onto Adhesion Superfrost Plus slide and cover slipped. The tissue was imaged with an Olympus upright microscope (BX51, Melville, NY) using appropriate excitation/emission filters for Alexa Fluor 488, Cy5, or a white light broadband filter to detect both anti-synuclein and the screened compounds simultaneously.

### *Cell Culture Models with Intracellular Alpha-Synuclein Inclusions*

Syn-T/Syn-1 model: H4 cells were maintained in culture, split to a four-chamber slide (Lab-Tek) and transfected using SuperFect Transfection Reagent (Qiagen) with DNA for synuclein-T and synphilin-1 to promote synuclein inclusion formation, as previously described [16]. Synphilin-1 is an alpha-synuclein interacting protein that co-localizes with the carboxy-terminal-truncated alpha-synuclein protein in separate cytoplasmic inclusions [17]. Transfected cells were kept in an incubator overnight to allow sufficient protein expression. The cells were then fixed with 4 % paraformaldehyde and treated with 1.5 % NGS/0.1 % Triton-X in PBS for 45 min at room temperature. Cells were immunostained with an anti-synuclein primary antibody (H3C, 1:1,000) in 1.5 % NGS in PBS for 2 h with shaking. Cells were washed with PBS, then incubated with fluorescent secondary antibody, either Alexa Fluor 488 or Cy5 (1:200 in PBS) for 1 h. Cells were washed with and stored in PBS at  $4^{\circ}\text{C}$ . Transfected cells were stained with

5  $\mu\text{M}$  of the test compound in PBS for 30 min, washed in PBS, and imaged with an Olympus BX51 upright microscope with a  $\times 60$ , NA=1.2 objective (Olympus Plan Neofluar, Thornwood, NY).

### *Alpha-Synuclein Fluorescence Complementation Cell Model*

H4 cells were maintained in culture, split to a four-chamber slide (Lab-Tek), and were co-transfected with DNA for an alpha-synuclein-dependent fluorescent protein complementation assay as previously described [18, 19]. The N-terminus half of VenusYFP fused to alpha-synuclein and a separate construct with the C-terminus half of VenusYFP fused to alpha-synuclein protein were co-transfected with SuperFect Transfection Reagent (Qiagen). When two or more alpha-synuclein proteins interact, the VenusYFP fluorescence is reconstituted from the non-fluorescent halves, and can be used as a marker for alpha-synuclein oligomerization. The appearance of fluorescence demonstrates at a minimum the formation of dimers of alpha-synuclein; however, higher molecular weight oligomers are also formed [18]. After fixation with 4 % paraformaldehyde in PBS, cells were incubated with 5  $\mu\text{M}$  of fluorescent ligand for 30 min in PBS at room temperature. Slides were rinsed with PBS three times and then imaged using an Olympus BX51 microscope with a  $\times 60$ , NA=1.2 objective (Olympus Plan Neofluar, Thornwood, NY).

### *Binding in Alpha-Synuclein-GFP Mouse Model*

Formalin-fixed 40- $\mu\text{m}$  sections from synuclein-eGFP mice expressing human alpha-synuclein fused to GFP under the platelet-derived growth factor beta (PDGF-b) promoter were used to evaluate the labeling of alpha-synuclein in a mouse model. In this mouse model, synuclein-GFP is expressed in a subset of cortical neurons and accumulates at pre-synaptic terminals [20, 21]. The free-floating tissue was incubated with 500 nM or 5  $\mu\text{M}$  of the imaging agent in PBS. Tissue sections were washed with PBS, mounted on a slide, and imaged using a Leica LCM confocal microscope at  $\times 63$  (Plan Apo, NA=1.2, Leica) with 488, 543, or 633 nm laser excitation and appropriate emission filters.

### *Specificity Over AD Pathology*

Paraffin-embedded paraformaldehyde (4 %)-fixed sections of the temporal lobe of neuropathologically verified human AD tissue were deparaffinized. Tissue sections were stained with 0.05 % thioflavin S (Sigma, St. Louis, MO) in 50 % ethanol for 5 min to visualize senile plaques and neurofibrillary tangles (NFT). The tissue was then incubated with 5  $\mu\text{M}$  of compound in PBS for 20 min at room temperature. Slides were rinsed in PBS, coverslipped, and then imaged on an Olympus BX51 microscope using a  $\times 20$  Plan Neofluar objective (NA=0.7, Olympus, Thornwood, NY), with a GFP emission filter for thioflavin S and appropriate emission ranges for each compound.

### *In Vivo Imaging for BBB Permeability*

Craniotomies in C57Bl/6J wildtype mice, 3–4 months old, were performed as previously described with minor modifications [22].

In brief, animals were anesthetized using 2 % isoflurane in balanced oxygen, and then a 5-mm diameter skull flap was removed. A craniotomy was performed, and the exposed brain area was covered by an 8-mm round glass coverslip, which was sealed to the skull with dental cement [22, 23]. This procedure allowed a transparent window into the mouse brain for use with *in vivo* microscopy of the cerebrovasculature. The mice were allowed 2–3 weeks for complete recovery after the craniotomy prior to imaging.

For imaging, the mice were anesthetized with 2 % isoflurane in balanced oxygen and secured in a custom stereotaxic frame, which fit into the microscope stage. Each imaging compound was solubilized in 1–6 % DMSO, 15 % Cremophor EL, and 1X PBS, and injected at a final concentration of 2–10 mg/kg. All *in vivo* imaging was performed using a custom-built epifluorescent microscope with a cooled CCD camera (Hamamatsu, ORCA-ER, C4742-80, Japan), objective (XFluor 2×/340, NA 0.14, Olympus, Japan), and appropriate excitation and emission filters for the compounds. Pre-injection images were taken, and then the solution of compound was injected IV (200–300  $\mu$ L) into the tail vein of the anesthetized mouse. A time course during and after the injection was taken for up to 60 min post-injection. The camera was controlled and images were acquired using Micro-Manager software [24] and analyzed using ImageJ [25].

## Results

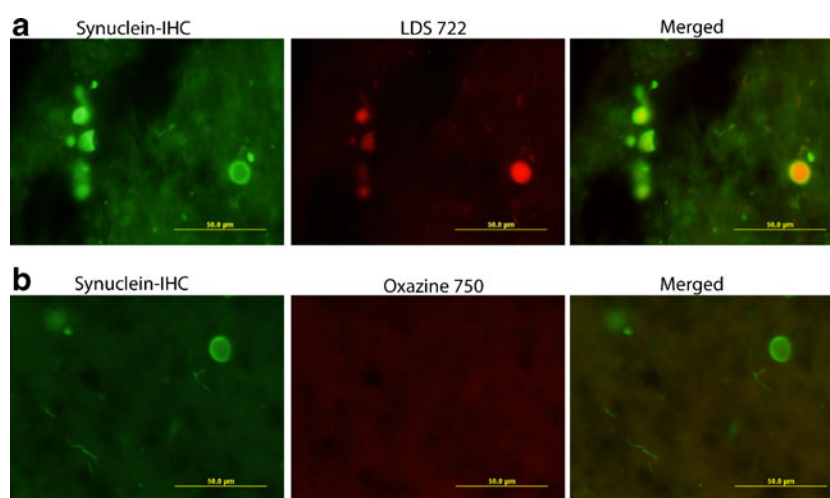
### *Specificity of Compounds for PD Pathology in Human Tissue*

To determine whether compounds exhibited specificity for alpha-synuclein pathology, the binding characteristics of the various imaging probes were tested by incubating the compounds with human DLB or PD tissue. Alpha-synuclein pathology was detected using immunohistochemistry with

an anti-synuclein antibody. Tissue was washed with PBS and then imaged using appropriate optical parameters. The compounds showed variable binding patterns to Lewy bodies and Lewy neurites. The imaging agents that bound Lewy bodies (+), but did not bind Lewy neurites (–), included 33'DTDCI, LDS-759, LDS-798, NIAD-1, Nile red, RD-01, THK-265, LDS-730, Nile blue, and HITC. Two probes, LDS-722 and Stilbene, showed specific staining of both LB and LN pathology, with a low amount of nonspecific background fluorescence (Fig. 1a). These results are summarized in Table 1. The majority of compounds screened did not show any specificity to alpha-synuclein pathology above nonspecific tissue fluorescence (Fig. 1b). The screened compounds that did not bind PD pathology are not reported in this study. Representative images are depicted in Fig. 1a, b.

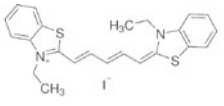
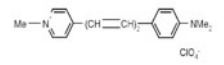
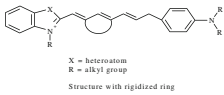
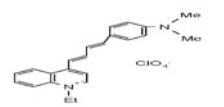
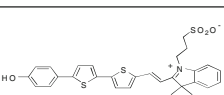
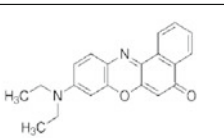
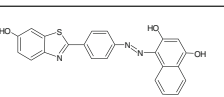
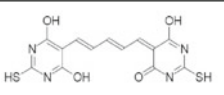
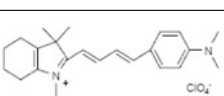
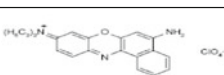
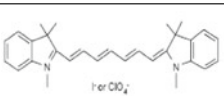
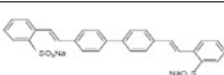
### *Labeling of Cell Culture Models of Alpha-Synuclein Accumulation*

The utility of two cell culture models of alpha-synuclein aggregation were evaluated for the purpose of developing a high-throughput screening assay for potential imaging agents. The first cell model forms alpha-synuclein inclusions when synuclein (Syn-T) and synphilin-1 are co-expressed [16]. H4 cells expressing Syn-T and Syn-1 were immunostained for alpha-synuclein and then incubated with the imaging probe. Cells were washed with PBS and imaged under appropriate optical conditions. Several compounds demonstrated labeling of H4-SynT/Syn-1 cells without any specificity for the synuclein oligomers. Other compounds did not show binding to



**Fig. 1.** Labeling of Lewy bodies (LB) and Lewy neurites (LN) in DLB postmortem midbrain tissue. **a** Shows positive staining (+) of Parkinson's disease (PD) pathology with compound LDS-722 (2  $\mu$ M). **b** Shows negative staining (–) of pathology with compound Oxazine 750 (5  $\mu$ M). The first image in each panel shows labeling of alpha-synuclein pathology with the H3C antibody and the secondary Alexa Fluor 488 (green). The circular LB is to the right in each image and LNs are to the left in the image. The second image shows the binding of the screened compound to the DLB tissue (red). The third image shows the two channels merged. A combination of a yellow–orange color indicates co-localization of alpha-synuclein with IHC and the screened compound.

**Table 1.** Summary of the screening results for lead compounds

Compound	Compound Structure	MW (Da)	EX (nm)	EM (nm)	LogP	PD LB	PD LN	Syn-GFP Mice	AD Plaq	AD NFT	BBB Cross
33'DTDCI		573	656	673	2.31	+	-	-	+	-	-
LDS-722		379	495	702	1.04	+	+	-	+	+	+
LDS-759*		515	558	736	2.88	+	-	+	-	-	+
LDS-798*		429	558	766	1.80	+	-	-	-	-	+
NIAD-1		550	540	720	1.52	+	-	-	+	+	+
Nile Red*		318	552	620	3.51	+	-	+	-	-	+
RD-01		413	600	615	1.39	+	-	-	+	-	+
THK-265		350	640	663	<1	+	-	-	+	-	-
LDS-730		430	603	668	1.54	+	-	-	+	+	+
Nile Blue*		417	624	660	1.41	+	-	+	-	-	+
HITC*		509	751	790	2.75	+	-	-	-	-	+
Stilbene		562	350	425	1.25	+	+	n/a	+	+	+

The first five columns identify several characteristics of each compound. The next five columns outline positive (+) and negative (-) binding to pathology in Parkinson's midbrain tissue and Alzheimer's temporal lobe tissue, and labeling of alpha-synuclein mouse models. The last column identifies compounds that crossed the BBB in vivo in wild-type mice ( $n = 3$  per compound). *MW* molecular weight in daltons, *EX* max excitation wavelength in nanometers, *EM* max emission wavelength in nanometers, *LogP* octanol/water partition coefficient to indicate lipophilicity, *PD LB* Lewy bodies in DLB tissue, *PD LN* Lewy neurites in DLB tissue, *AD Plaq* senile plaque labeling in AD tissue, *AD NFT* neurofibrillary tangle labeling in AD tissue, *BBB* cross ability to penetrate the blood brain barrier in vivo

\*Lead compounds with alpha-synuclein specificity

*n/a* Not evaluated in the assay

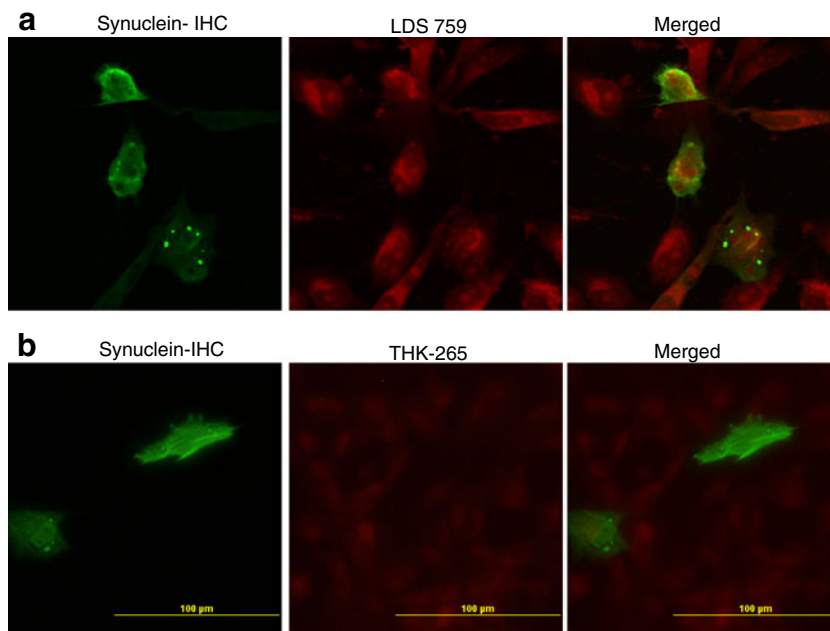


**Fig. 2.** Compounds are not specific to alpha-synuclein-T/synphilin-1 intracellular inclusions or alpha-synuclein-expressing H4 cells. **a** Shows LDS-759 (5 μM) as a representative positive labeling of all cells. **b** Shows THK-265 (5 μM) as a representative compound that did not label any cells. None of the compounds bound to alpha-synuclein–synphilin intracellular inclusions. The first image shows fluorescence of alpha-synuclein with H3C antibody in transfected cells (*green*). The second image (*red*) shows fluorescence of the imaging probe. The third image shows the two channels merged. There is no overlap of probe and alpha-synuclein IHC on inclusions or specific to alpha-synuclein-transfected cells.

either the cells or the inclusions. Representative images are shown in Fig. 2.

The second cell culture model uses a protein complementation assay to detect alpha-synuclein oligomers in cells. H4 cells co-expressed alpha-synuclein fused to N-terminal-VenusYFP and alpha-synuclein fused to C-terminal–

VenusYFP. The YFP fluorescence is reconstituted when two or more alpha-synuclein proteins interact [18, 19]. Cells were incubated with imaging probes, washed with PBS, and imaged under appropriate conditions, as described above. Similar results were obtained with this cell culture model; there was no specific labeling of the alpha-synuclein

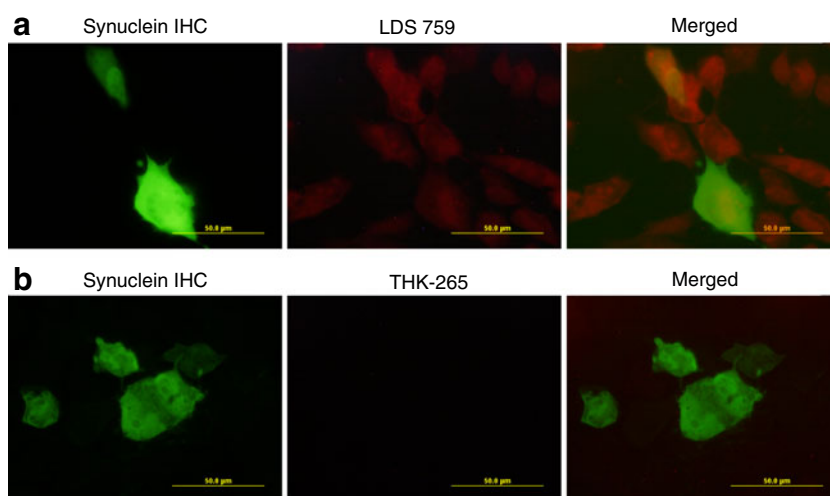


**Fig. 3.** The compounds did not specifically label VenusYFP–synuclein-transfected H4 cells. **a** Illustrates a representative image of compound, LDS-759 (5 μM), which labeled all cells, transfected and non-transfected. **b** Shows THK-265 (5 μM), a probe that did not label any cells. The first image shows alpha-synuclein YFP fluorescence (*green*) in cells, the second image shows probe fluorescence (*red*), the third image shows the two channels merged (*yellow* indicates co-localization). None of the compounds bound specifically to only the transfected cells, indicating that the compounds were not specific to the alpha-synuclein species expressed in the cells.

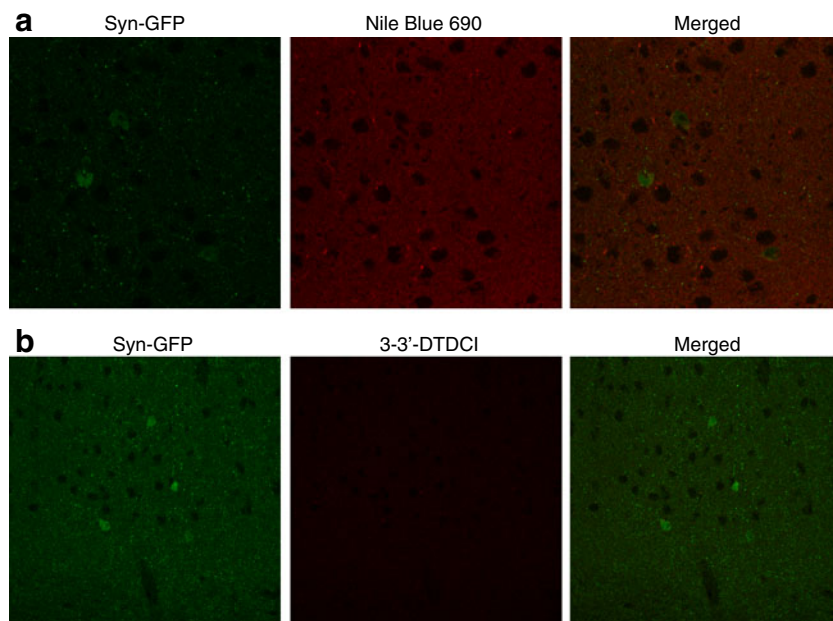


**Fig. 4.** Compounds are not specific to the alpha-synuclein aggregates in synuclein-GFP expressing neurons of transgenic mouse cortical tissue. Syn-GFP is present at the synaptic terminals, shown as punctate fluorescence in the images and expressed in the soma of about 1 % of cortical neuron [20, 21]. **a** Illustrates a representative image of nonspecific labeling of mouse cortical tissue by Nile blue 690 (500 nM). Probe 3-3'DTDCI (500 nM) demonstrates a representative image of negative labeling or the absence of fluorescence in transgenic mouse cortical tissue. **b** The first images in both panels show the distribution of synuclein-GFP in the cortex of the transgenic mouse brain. The second image shows the fluorescence (*red*) of the screened compound on the same cortical tissue. These images show that there is no specific labeling of either compound to the alpha-synuclein expressed in the Syn-GFP transgenic mouse model.

oligomers in the Syn-YFP cells with compounds that bound to the Lewy bodies in human tissue. Representative images are shown in Fig. 3. These cell culture models of alpha-synuclein accumulation did not predict binding to

neuropathologically identified Lewy bodies found in the human brain. These results may be due to the non-fibrillar nature of alpha-synuclein oligomers in these cell culture models.

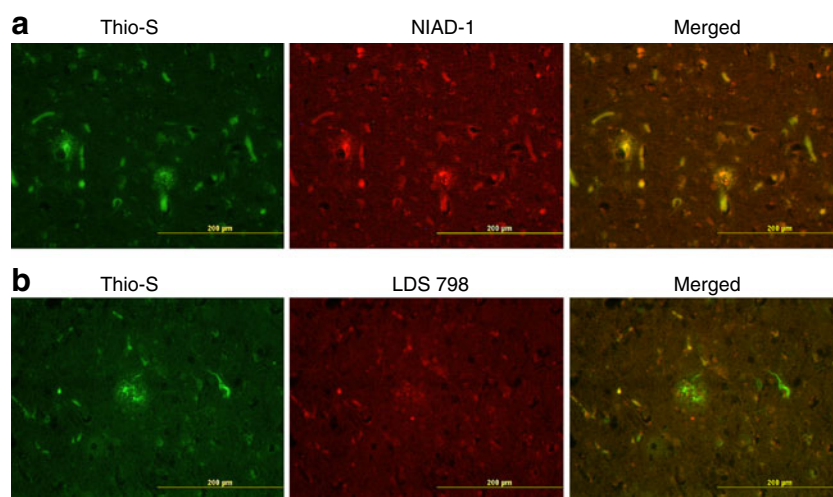


**Fig. 5.** The candidate imaging agents showed varied labeling patterns of senile plaques and neurofibrillary tangles in Alzheimer's disease temporal lobe tissue. **a** Demonstrates that compounds that bound to Lewy Bodies like NIAD-1 (5  $\mu$ M) also bound to amyloid plaques and tau neurofibrillary tangles. **b** Shows LDS-798 (5  $\mu$ M), which did not bind to either plaques or tangles in AD. The first image in each panel is AD tissue labeled with 0.05 % thioflavin S (*Thio-S*). The second image shows the fluorescence (*red*) of the screened compound on the tissue. The final image in each panel is a merged view of Thio-S and the compound on AD pathology. A combination of a *yellow-orange* color indicates co-localization of Thio-S and the compound, as seen with NIAD-1 on plaques and tangles in panel **a**.

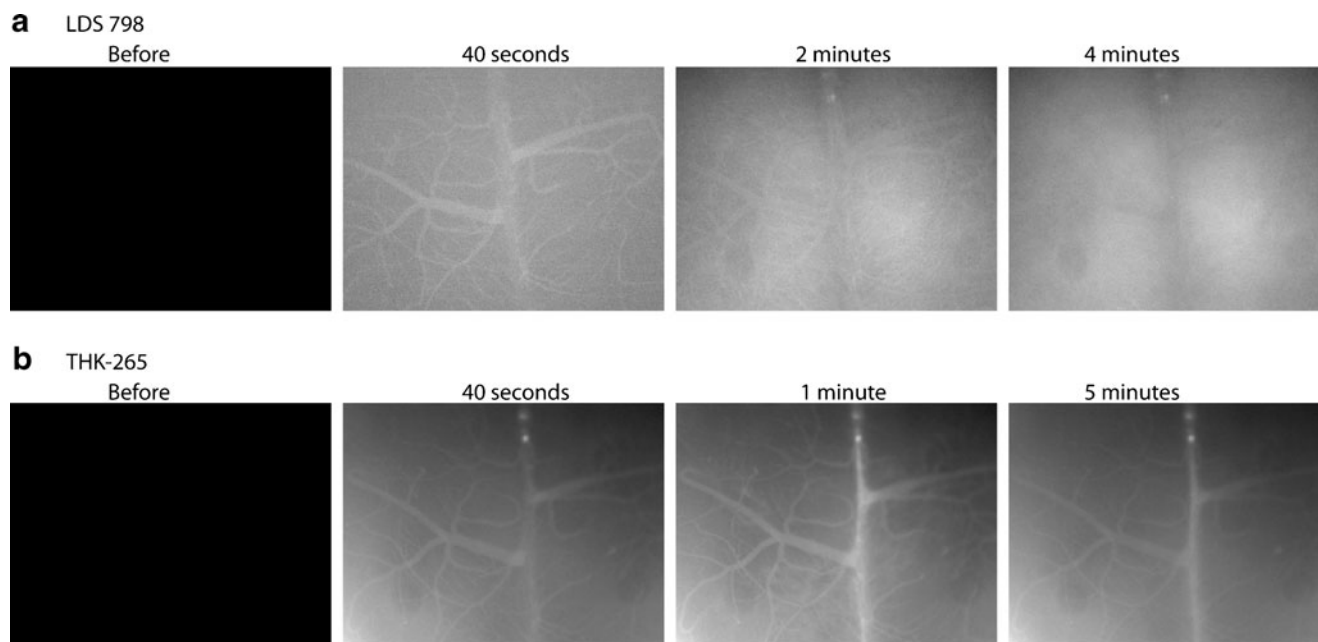


**Fig. 6.** Real-time imaging in wildtype mice, showing blood–brain barrier permeability time courses for representative compounds after intravenous tail vein injection. The first image in each panel shows the brain prior to injection of the compound. The subsequent images are selected points from the time series. **a** Illustrates a time course of LDS-798 (4 mg/kg) crossing the blood–brain barrier into the parenchyma and clearing from the cerebrovasculature within 4 min. **b** A time course of THK-265 (4 mg/kg) appearing in the cerebrovasculature; subsequent images demonstrate that it does not detectably cross into the brain parenchyma within 5 min. THK-265 shows a steady signal in the vasculature throughout the time series, up to 60 min (not shown).

### *Labeling of Alpha-Synuclein Pathology in a Mouse Model*

The utility of an alpha-synuclein mouse model as an additional screening tool for *in vivo* analysis of imaging probes was evaluated. In the Syn-GFP mouse model, an alpha-synuclein–GFP fusion protein, under a PDGF promoter, is expressed in 1 % of cortical neurons and shows localization at pre-synaptic terminals [20, 21]. To determine if any of the compounds demonstrated binding to Syn-GFP neurons, 40- $\mu$ m sections of tissue were incubated with the imaging probes. The tissue was washed with PBS and optical imaging was performed under appropriate conditions. None of the compounds showed selective binding to the Syn-GFP expressing neurons or alpha-synuclein localized at synapses. Some compounds bound non-specifically to cellular membranes, while others showed no evidence of binding. Representative images are shown in Fig. 4.

### *Selectivity over Alzheimer's Pathology in Human AD Tissue*

To determine the specificity of our compounds for alpha-synuclein pathology, lead candidates were screened for binding to senile plaques and NFT, the main pathological hallmarks of Alzheimer's disease. Human AD tissue was stained with 0.05 % thioflavin S and then incubated the

imaging probes individually on the tissue. The compounds showed various binding patterns to AD pathology. A few compounds had positive staining and bound both amyloid-beta plaques and NFT. Several imaging agents bound to plaques but not tangles. A few compounds did not bind either pathology. These results are summarized in Table 1. Probes LDS-759, LDS-798, Nile blue, HITC, and Nile red did not label amyloid or tau pathology in the human AD tissue. This suggests that these five compounds show some selectivity for Lewy pathology in human tissue. Representative images are shown in Fig. 5a, b.

### *BBB Permeability of Screened Compounds*

Compounds that bound to PD pathology were further assessed for BBB permeability with intravital microscopy. Anesthetized mice ( $n=3$  per compound) were administered compounds via IV injection through a tail vein at 2–10 mg/kg of ligand. Optical imaging was performed to monitor the fluorescent molecule in the cerebrovasculature. A time course after an IV injection of each compound was obtained. An agent that crossed the BBB was first fluorescent in the cerebrovasculature and then showed progressive leakage from the vasculature into the parenchyma. Agents that did not exhibit BBB penetration remained fluorescent in the vasculature over time and did not appear to change location. Several of the compounds tested including, LDS-722, Nile



blue, and LDS-798, showed BBB permeability. Moreover, the majority of compounds that crossed the BBB also cleared from the cerebrovasculature within 10 min. Ligands that did not traverse the BBB remained fluorescent in the vasculature for an extended period of time and were imaged for up to 1 h. These data are also included in Table 1. Representative time series images are shown in Fig. 6.

## Discussion

PD is a progressive neurodegenerative disease that would benefit from noninvasive biomarkers for alpha-synuclein pathology, which would permit early diagnosis and provide a quantitative endpoint for clinical trials. Molecular imaging in AD has benefited from advances in probe design leading to PET imaging of amyloid deposits in AD patients. PiB and florbetapir have permitted longitudinal imaging of the natural progression of amyloid deposition and are currently being used as an outcome measure in clinical trials of therapeutic agents [26]. This success has encouraged the development of molecular imaging agents targeting the pathological aggregates of alpha-synuclein found in PD.

PD is characterized by the presence of LB and LN. Currently, little is known about how or why these distinctive aggregates form. It has been established that small diffusible oligomers of alpha-synuclein play a role in cytotoxicity, and evidence suggests that the larger alpha-synuclein aggregates may even be neuroprotective [18]. Thus, while LB and LN are the most obvious target as an imaging biomarker, it has yet to be established if they will be the most relevant or informative target. The most useful imaging probe would probably be one that reports both Lewy aggregates and smaller diffusible oligomers. This approach would increase sensitivity by detecting a broader range of targets.

A small library of compounds was screened as putative molecular imaging ligands for Lewy pathology. The compounds have desirable physicochemical properties permitting reasonable solubility, and the potential to cross the blood–brain barrier when administered systemically. Using real-time intravital microscopy, it was determined that some of these compounds could enter the brain with promising kinetics. Thus, it was determined that it is possible to identify molecular imaging agents that could be suitable for testing in humans.

Despite the recent success of amyloid targeting PET agents, the development of CNS targeting probes is extremely difficult. The blood–brain barrier is a major obstacle and limits the size of the small molecule agent to <600 MW. Likewise, lipophilicity is a major determinant of passive blood–brain barrier entry. The lipophilicity of successful small molecule imaging agents, as defined by logP (octanol–water partition index), is limited to a range between ~1 and 3 [27]. Our lead compounds were of low molecular weight and had logP values that mostly fell within this range.

The results from the cell culture and animal models of alpha-synuclein overexpression were surprising. The intent of the cell culture experiments was to enable a higher throughput approach to screening fluorescent ligands; however, none of the compounds that bound to alpha-synuclein pathology in the human brain tissue sections bound to the oligomers or inclusions in the cell culture models. Thus, the cell-based models were not predictive of binding patterns to bona fide Parkinson's disease pathology. This suggests that solely overexpressing the alpha-synuclein protein in cells for a few days does not accurately model the complex 3D structure of alpha-synuclein containing LBs, which likely takes years to form.

The same lack of specific binding was observed in the transgenic mouse model overexpressing alpha-synuclein, despite the presence of high molecular weight species and continuous expression of the human protein over the animal's life span. This result was confirmed in tissue from virally induced alpha-synuclein expression in rats (data not shown). One possible explanation for the lack of detectable binding in the cell culture models, transgenic mouse model, and virally-induced rat model is a low-affinity binding of the ligands combined with an assay that lacks sensitivity compared with other approaches. The simplest explanation for the lack of binding in these synuclein expressing models is that they lack fibrillar forms of the protein aggregates, which would more closely resemble the conformation found in Lewy bodies. Together, these data suggest that there is much to learn about alpha-synuclein aggregation, and that the field would substantially benefit from a more relevant cell and animal model of PD. Finally, we believe that specificity for Lewy bodies and Lewy neurites, and not just alpha-synuclein aggregates, is the relevant target for clinical imaging in PD patients.

A major confound for specific detection of LB pathology is the common coexistence of amyloid aggregates in PD patients. Amyloid plaques are large extracellular deposits that can occupy up to several percent of local brain volume. Therefore, it will be critical to have an imaging ligand that displays selectivity over amyloid pathology. Since there are no crystal structures yet to allow rational design of ligands for either LB or senile plaques, our library was screened for binding to amyloid plaques in human tissue from AD cases. Most amyloid binding reagents are not specific for amyloid-beta aggregates but prefer the beta-sheet structure of protein aggregates common to both alpha-synuclein and amyloid. Despite this, several compounds were identified that showed specificity for LB over amyloid plaques. This result suggests that it is possible to identify a probe that will not “cross react” with Alzheimer pathology.

Our fluorescence-based assays and intravital microscopy tools allowed us to characterize the pharmacokinetics of our lead compounds in the mouse brain. While largely qualitative, this approach allowed us to monitor the appearance of the compound in the cerebrovasculature during IV injection, and watch in real time as the compound crossed or did not cross the blood–brain barrier. Similarly, the images allowed us to follow the clearance of compound from both the brain

parenchyma and the circulation over time. An ideal PET ligand would enter the brain in sufficient amounts and then be cleared from the brain and circulation very quickly to allow specific detection of probe that is bound to target. Because our compounds do not bind to oligomers in the animal model of alpha-synuclein expression, we were not able to observe brain entry and alpha-synuclein staining *in vivo*. Nonetheless, our *in vivo* imaging results demonstrate that it is possible to identify a compound that binds to PD pathology and has the physicochemical properties consistent with brain penetration.

A key property of any imaging ligand is affinity for the target. While the affinities of the compounds for LB pathology in fixed human tissue sections was not measured, the optical contrast was qualitatively rated as an estimate of the degree of binding. Additionally, as formalin-fixed tissue was used to increase throughput in the screening approach, it is possible that fresh frozen tissue sections would have led to different binding properties and potentially led to more suitable reagents. Regardless, it will be important to evaluate the suitability of the putative imaging agents in humans.

It would be desirable to develop a predictive model of alpha-synuclein aggregation that is compatible with standard competitive binding techniques to quantitatively determine the affinity of our compounds. While numerous approaches for using recombinant alpha-synuclein aggregates have been described, it is not clear that any of these formulations will represent the binding observed to LB in human tissue. Likewise, a competitive binding assay requires a gold standard compound to compete with, and to date that would be either Thioflavin T or Thioflavin S. Both of these compounds bind with very low contrast to LB pathology and thus are probably very low affinity binders. Therefore, one of the outcomes of this current work is the demonstration of putative alpha-synuclein binding compounds that could become a benchmark for evaluating alpha-synuclein aggregate formulations as well as first generation tools towards identifying high-affinity binding sites.

In summary, using fluorescence-based screening of a small library of fluorescent compounds several lead compounds were identified as candidates for molecular imaging of LB pathology in PD patients. These compounds show specificity for alpha-synuclein pathology over amyloid pathology in human tissue sections, have low molecular weights, logP values that are consistent with good brain entry, and do, in fact, cross the blood-brain barrier. Thus, these compounds represent proof in concept that a PD molecular imaging agent can be developed and should at least serve as starting points for optimized probe development. For clinical imaging using PET, these compounds will need to be radiolabeled and their biodistribution and pharmacokinetics evaluated more rigorously. It will also be important to evaluate these compounds for toxicity. Ultimately, these contrast agents or similar compounds hold the potential to monitor Parkinson's disease pathology longitudinally and allow correlation of these changes with the onset

and progression of symptoms. Additionally, a successful compound would provide an ideal quantitative end point for analyzing therapeutics aimed at eliminating the main pathological aggregates of PD.

*Acknowledgments.* Many thanks to Julia George, University of Illinois, for the H3C Antibody and to Eliezer Masliah, UCSD, for the Syn-GFP mouse model.

*Funding.* Michael J. Fox Foundation and NIH AG026240.

*Conflict of Interest.* The authors declare that they have no conflict of interest.

## References

- de Lau LM, Breteler MM (2006) Epidemiology of Parkinson's disease. *Lancet Neurol* 5:525–535
- Stoessl AJ (2012) Neuroimaging in Parkinson's disease: from pathology to diagnosis. *Parkinsonism Relat Disord* 18(Suppl 1):S55–9
- Varrone A, Toth M, Steiger C et al (2011) Kinetic analysis and quantification of the dopamine transporter in the nonhuman primate brain with 11C-PE2I and 18F-FE-PE2I. *J Nucl Med* 52:132–139
- Sasaki T, Ito H, Kimura Y et al (2012) Quantification of dopamine transporter in human brain using PET with 18F-FE-PE2I. *J Nucl Med* 53:1065–1073
- Varrone A, Hallidin C (2010) Molecular imaging of the dopamine transporter. *J Nucl Med* 51:1331–1334
- Hurley MJ, Mash DC, Jenner P (2003) Markers for dopaminergic neurotransmission in the cerebellum in normal individuals and patients with Parkinson's disease examined by RT-PCR. *Eur J Neurosci* 18:2668–2672
- Bacskaï BJ, Hickey GA, Skoch J et al (2003) Four-dimensional multiphoton imaging of brain entry, amyloid binding, and clearance of an amyloid-beta ligand in transgenic mice. *Proc Natl Acad Sci U S A* 100:12462–12467
- Klunk WE, Engler H, Nordberg A et al (2004) Imaging brain amyloid in Alzheimer's disease with Pittsburgh Compound-B. *Ann Neurol* 55:306–319
- Klunk WE, Engler H, Nordberg A et al (2003) Imaging the pathology of Alzheimer's disease: amyloid-imaging with positron emission tomography. *Neuroimaging Clin N Am* 13:781–789
- Klunk WE, Lopresti BJ, Ikonomic MD et al (2005) Binding of the positron emission tomography tracer Pittsburgh compound-B reflects the amount of amyloid-beta in Alzheimer's disease brain but not in transgenic mouse brain. *J Neurosci* 25:10598–10606
- Mathis CA, Mason NS, Lopresti BJ, Klunk WE (2012) Development of positron emission tomography beta-amyloid plaque imaging agents. *Semin Nucl Med* 42:423–432
- McKeith IG, Galasko D, Kosaka K et al (1996) Consensus guidelines for the clinical and pathologic diagnosis of dementia with Lewy bodies (DLB): report of the consortium on DLB international workshop. *Neurology* 47:1113–1124
- Cantuti-Castelvetri I, Klucken J, Ingelsson M et al (2005) Alpha-synuclein and chaperones in dementia with Lewy bodies. *J Neuropathol Exp Neurol* 64:1058–1066
- Mathis CA, Wang Y, Holt DP et al (2003) Synthesis and evaluation of 11C-labeled 6-substituted 2-arylbenzothiazoles as amyloid imaging agents. *J Med Chem* 46:2740–2754
- Payton JE, Perrin RJ, Clayton DF, George JM (2001) Protein-protein interactions of alpha-synuclein in brain homogenates and transfected cells. *Brain Res Mol Brain Res* 95:138–145
- McLean PJ, Kawamata H, Hyman BT (2001) Alpha-synuclein-enhanced green fluorescent protein fusion proteins form proteasome sensitive inclusions in primary neurons. *Neuroscience* 104:901–912
- Wakabayashi K, Engelender S, Yoshimoto M et al (2000) Synphilin-1 is present in Lewy bodies in Parkinson's disease. *Ann Neurol* 47:521–523
- Outeiro TF, Putcha P, Tetzlaff JE et al (2008) Formation of toxic oligomeric alpha-synuclein species in living cells. *PLoS One* 3:e1867
- Danzon KM, Ruf WP, Putcha P et al (2011) Heat-shock protein 70 modulates toxic extracellular alpha-synuclein oligomers and rescues trans-synaptic toxicity. *FASEB J* 25:326–336

20. Unni VK, Weissman TA, Rockenstein E et al (2010) *In vivo* imaging of alpha-synuclein in mouse cortex demonstrates stable expression and differential subcellular compartment mobility. *PLoS One* 5:e10589
21. Rockenstein E, Schwach G, Ingolic E et al (2005) Lysosomal pathology associated with alpha-synuclein accumulation in transgenic models using an eGFP fusion protein. *J Neurosci Res* 80:247–259
22. Skoch J, Hickey GA, Kajdasz ST et al (2005) *In vivo* imaging of amyloid-beta deposits in mouse brain with multiphoton microscopy. *Methods Mol Biol* 299:349–363
23. Spires-Jones TL, de Calignon A, Meyer-Luehmann M et al (2011) Monitoring protein aggregation and toxicity in Alzheimer's disease mouse models using *in vivo* imaging. *Methods* 53:201–207
24. Edelstein A, Amodaj N, Hoover K, et al. (2010) Computer control of microscopes using microManager. *Curr Protoc Mol Biol* Chapter 14:Unit14.20
25. Schneider CA, Rasband WS, Eliceiri KW (2012) NIH Image to ImageJ: 25 years of image analysis. *Nat Methods* 9:671–675
26. Swaminathan S, Shen L, Risacher SL et al (2012) Amyloid pathway-based candidate gene analysis of [(11)C]PiB-PET in the Alzheimer's Disease Neuroimaging Initiative (ADNI) cohort. *Brain Imaging Behav* 6:1–15
27. Dishino DD, Welch MJ, Kilbourn MR, Raichle ME (1983) Relationship between lipophilicity and brain extraction of C-11-labeled radiopharmaceuticals. *J Nucl Med* 24:1030–1038